

Field and intensity correlation in random media

P. Sebbah,¹ R. Pnini,² and A. Z. Genack³

¹*Laboratoire de Physique de la Matière Condensée, CNRS UMR 6622, Université de Nice-Sophia Antipolis, Parc Valrose, 06108 Nice Cedex 02, France*

²*Technion-Israel Institute of Technology, 32000 Haifa, Israel*

³*Department of Physics, Queens College of the City University of New York, Flushing, New York 11367*

(Received 7 March 2000)

We have obtained the spectral and spatial field correlation functions, $C_E(\Delta\omega)$ and $C_E(\Delta x)$, respectively, from measurement of the microwave field spectrum at a series of points along a line on the output of a random dielectric medium. $C_E(\Delta\omega)$ and $C_E(\Delta x)$ are shown to be the Fourier transforms, respectively, of the time of flight distribution, obtained from pulsed measurements, and of the specific intensity. Unlike $C_E(\Delta\omega)$, the imaginary part of $C_E(\Delta x)$ is shown to vanish as a result of the isotropy of the correlation function in the output plane. The complex square of the field correlation function gives the short-range or C_1 contribution to the intensity correlation function C . Longer-range contributions to the intensity correlation function are obtained directly by subtracting C_1 from C and are in good agreement with theory.

PACS number(s): 41.20.Jb, 05.40.-a, 71.55.Jv

The random phasing of multiply scattered partial waves in disordered media leads to intensity fluctuations whose short-range spatial correlation is determined by the square of the field correlation function. This field-factorization term is the leading or C_1 contribution to the cumulant intensity correlation function $C = \langle \delta I \delta I' \rangle \sim C_1 = |\langle EE'^* \rangle|^2$. Here δI is the fluctuation of the intensity I from its ensemble average value, $\delta I = I - \langle I \rangle$, E is the electromagnetic field, and $\langle \dots \rangle$ represents the ensemble average. This approximation gives the well-known Gaussian statistics of the field [1,2] and the negative exponential distribution of the intensity [3–5]. The intensity correlation length δx sets the scale of the speckle spots, while the correlation frequency $\delta\nu$ represents the inverse of the spread in transit time between the source and the point of observation. Recent advances in speckle statistics have shown, however, that fluctuations in intensity [5–10], total transmission [8,11–17], and conductance [18–22] are enhanced beyond the predictions of Gaussian statistics, as a result of long- and infinite-range intensity correlations, the C_2 and C_3 contributions to the intensity correlation function, respectively.

In this paper, we present observations of the field correlation function $\langle EE'^* \rangle$ in the spectral and spatial domains in measurements of the microwave field transmitted through random media. We relate these to their corresponding Fourier transforms, the time of flight distribution of photons, and the specific intensity, which gives the angular distribution of the intensity in the far field. Taking the complex square of the field correlation function gives the C_1 contribution and makes it possible to consider the difference $C - C_1$, which includes only terms beyond the field-factorization approximation, which are responsible for enhanced fluctuations of transmission quantities. Since higher order contributions than C_2 are small in these samples, $C - C_1$ essentially equals C_2 . In the past C_2 was found from measurements of the correlation function of total transmission [14,15] or from fitting the measured intensity correlation function using an assumed functional form for C_1 and C_2 [23]. Here C_2 is directly separated from the intensity correlation function by subtracting C_1 from C . Theoretical expressions for C_1 and C_2 in the

frequency domain including absorption and boundary conditions are in good agreement with experiments.

In order to eliminate instrumental distortions of field and intensity spectra, we normalize the field by the square root of the average intensity and the intensity by its average value at each frequency and position. In addition, measurements are carried out in a frequency range in which the change in scattering parameters is small. This allows us to obtain the functional form of the relative degree of correlation. We will henceforth denote the normalized intensity $I/\langle I \rangle$ by I and the normalized field $E/\langle I \rangle^{1/2}$ by E . The cumulant correlation function of the normalized intensity will now be denoted by C , which is the sum of three terms [24,25,12,13]:

$$C = C_1 + C_2 + C_3. \quad (1)$$

The C_1 term is unity for frequency shift $\Delta\nu = 0$ and displacement $\Delta x = 0$. The spectral field correlation function for a plane wave incident upon a slab or upon a quasi-one-dimensional sample is given by [26–29]

$$C_E(\Delta\nu) = \langle E(\nu)E^*(\nu + \Delta\nu) \rangle = \frac{\sinh q_0 a}{\sinh q_0 L'} \frac{\sinh \alpha L'}{\sinh \alpha a}, \quad (2)$$

where L is the sample length, $L' = L + 2z_b$ is the effective length corrected for internal reflection, $z_b = 2l(1+R)/(1-R)$ is the extrapolation length [30–32], R is the reflection coefficient at the boundary averaged over internal incident angles, l is the transport mean free path, $\alpha = 1/L_a$ is the inverse of the diffusive absorption length $L_a = \sqrt{D}\tau_a$, D is the diffusion constant, τ_a is the absorption time, $a = 5l/3$ is the randomization distance from the plane in which the intensity inside the medium extrapolates to zero, $q_0 = \gamma_+ - i\gamma_-$, $\gamma_{\pm}^2 = \frac{1}{2}(\sqrt{\alpha^4 + \beta^4} \pm \alpha^2)$, and $\beta = \sqrt{2\pi\Delta\nu/D}$. The C_2 term is of order $1/g$ at $\Delta\nu = 0$ and $\Delta x = 0$. Far from the localization transition, the expression for the C_2 contribution including absorption is given by [33,34]

$$C_2(\Delta\nu) = \frac{4}{gL} \frac{\sqrt{\alpha^4 + \beta^4}}{\beta^4} \times \frac{\gamma_+ \sinh(2\gamma_+L) - \gamma_- \sin(2\gamma_-L) - \alpha \sinh(2\alpha L)}{\cosh(2\gamma_+L) - \cos(2\gamma_-L)}, \quad (3)$$

where $g = Ak_0^2 l / 3\pi L$ is the ensemble averaged dimensionless conductance for a tube of length L and cross section A . This expression differs from Eq. (14) in [33] by a factor of 2 to take into account the one-channel-in, one-channel-out measurement described below. Thus,

$$C_2(\Delta\nu=0) = \frac{\sinh 2\alpha L - 2\alpha L(2 - \cosh 2\alpha L)}{4g\alpha L \sinh^2(\alpha L)}. \quad (4)$$

In the absence of absorption, $C_2(\Delta\nu) = 4/3g$. Equations (3) and (4) do not include internal reflection. The complete expression for C_2 including internal reflection is detailed in Appendix A. The C_3 contribution is responsible for the universal conductance fluctuations measured in electronic systems [18–21]. It has recently been observed in optics in time correlation experiments [35]. This contribution is of order $1/g^2$ and is more strongly suppressed by absorption than the C_2 term [8] and will therefore not be considered here.

The system studied here is composed of randomly positioned $\frac{1}{2}$ -inch polystyrene spheres at a volume filling fraction of 0.52 contained within a 1 m long, 7.6 cm diameter copper tube. Wire antennas are used as the emitter and detector at the input and output surfaces of the sample. A Hewlett-Packard 8722C vector network analyzer is used to measure the microwave field, giving its amplitude and phase. Measurements are made in the Ku and K bands with frequency steps of 625 kHz and displacements of 1 mm along a 4 cm line running symmetrically about the center of the output surface. After the spectrum is taken at a given position, the detector is translated by 1 mm. Measurements are made for two positions of the input antenna separated by 3 cm. Once spectra are taken at each point on the line, the copper tube is rotated briefly to create a new configuration. Measurements are made in 200 sample realizations and spectral and spatial correlation functions are computed from these data.

The real and imaginary parts of the field correlation function with frequency shift are shown in Fig. 1. Averaging has been performed over sample configuration, position of the source and detector, and frequency between 16.8 and 17.8 GHz, where transport parameters are known to vary slowly [32]. The real part of the correlation function falls quadratically, whereas the imaginary part rises linearly with frequency shift, for small shifts [36]. From a three-parameter fit using Eq. (2) and the value of the reflection coefficient $R = 0.13$ measured in [32], we find the diffusion constant $D = 3.3 \times 10^{10}$ cm²/s, the absorption length $L_a = 33.3$ cm, and the penetration depth $a = 18.3$ cm, which in turn give the extrapolation length $z_b = 9.5$ cm and the mean free path $l = 11.0$ cm.

We have also carried out measurements of pulsed propagation in the same sample. The response to a 1 ns pulse shaped by a pulse forming network and mixed to a local oscillator at 19 GHz is measured using high bandwidth B&H

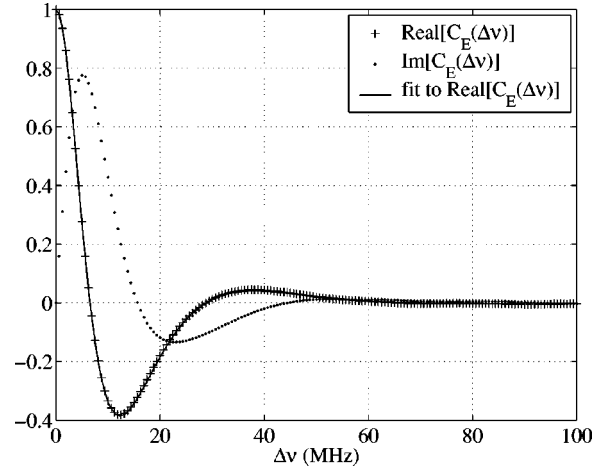


FIG. 1. Real (crosses) and imaginary (dots) part of field correlation function with frequency shift. Equation (2) has been used to fit (solid line) the real part. The fit to the imaginary part is not shown, but it necessarily follows.

Electronics amplifiers. The results are collected using a digital sampling oscilloscope. The complex square is taken and averaged over 4096 configurations and shown in Fig. 2. Because the incident pulse is much shorter than the typical traversal time through the medium, and encompasses a bandwidth much greater than the correlation frequency, this measurement gives the time of flight distribution of photons propagating through the sample at a carrier frequency of 19 GHz. The line through the data is the Fourier transform of the field correlation function which is averaged over configuration and frequencies between 18.5 and 19.5 GHz. The agreement between these sets of data shows that the field correlation function and the time of flight distribution are Fourier transform pairs in agreement with the demonstration in Appendix B. This result is analogous to the demonstration that the intensity distribution on the output surface due to point excitation (the point spread function) and the intensity correlation function with identical shifts in the incident and scattered wave vector [12,37] are Fourier transform pairs

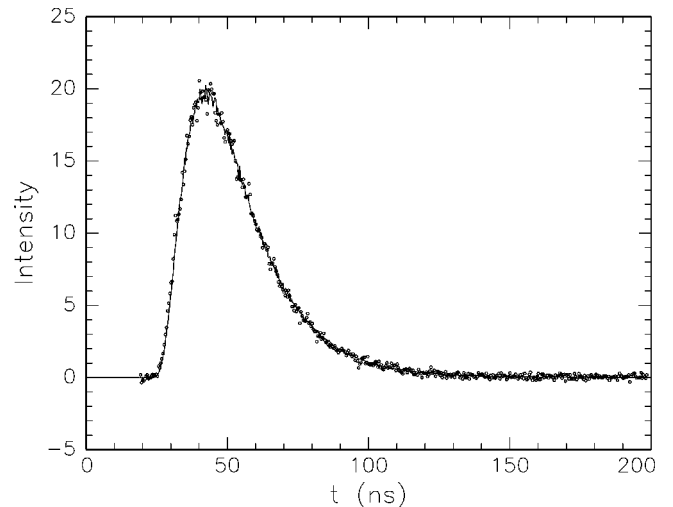


FIG. 2. Time of flight distribution for carrier frequency 19 GHz. The continuous line is the Fourier transform of the field correlation function [Eq. (B4)] in the range 18.5 to 19.5 GHz.

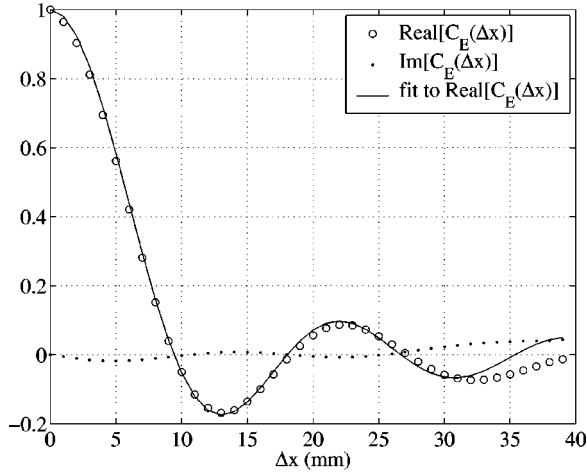


FIG. 3. Real (circles) and imaginary (dots) part of field correlation function with displacement. Equation (6) has been used to fit (solid line) the real part. The imaginary part is predicted to vanish.

[38]. In both cases the variables of the incident and outgoing waves are shifted by the same amount. This result holds even in the presence of significant long-range intensity correlation. In previous optical studies [26], only the intensity was measured. Its correlation function with frequency was shown to be the square of the Fourier transform of the time of flight distribution. In that case, long-range correlation was negligible and the measured correlation function was essentially equal to C_1 .

The real and imaginary parts of the field correlation function with displacement $C_E(\Delta x) = \langle E(x, \nu) E^*(x + \Delta x, \nu) \rangle$ averaged over sample configuration, frequency ν between 18 and 18.5 GHz, and position x , are shown in Fig. 3. The imaginary part of the field correlation function with displacement is small, in contrast to the field correlation function with frequency (see Fig. 1). As shown below, this is a consequence of the isotropy of the random field. Such isotropy may be expected at the output of a quasi-one-dimensional sample, far from the boundary, or on length scales smaller than the sample thickness at the output of a random slab. By the translational invariance of the field correlation function with displacement, $C_E(\Delta x) = \langle E(x) E^*(x + \Delta x) \rangle = \langle E(x - \Delta x) E^*(x) \rangle = C_E^*(-\Delta x)$. By the isotropy of $C_E(\Delta x)$ with regard to the direction of the displacement, we can exchange $-\Delta x$ and Δx . This gives $C_E(\Delta x) = C_E^*(\Delta x)$. Since $C_E(\Delta x)$ equals its complex conjugate, its imaginary part vanishes. In contrast, the imaginary part of the field correlation function with frequency shift $C_E(\Delta \omega)$ does not vanish because the change of $\Delta \omega$ to $-\Delta \omega$ also requires that the complex conjugate be taken.

In transmission, the angular distribution of the scattered intensity is predicted to be [39]

$$I(\theta) = \Delta \cos \theta + \cos^2 \theta, \quad (5)$$

where $\Delta = z_b/l$ and the scattering angle θ is measured from the normal to a reference plane Σ close to the output surface. Following Ref. [39], the two-dimensional (2D) Fourier transform of this expression is the 2D spatial correlation function of the field over Σ . When taken along a line, this reduces to

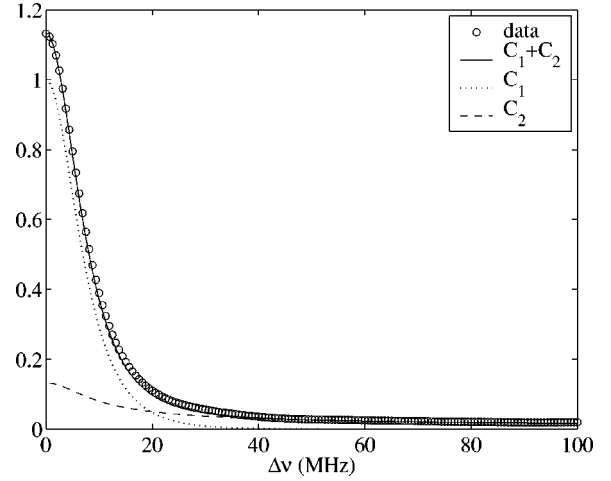


FIG. 4. Intensity correlation function with frequency shift (circles). The solid line is the theoretical expression for $C_1 + C_2$ using the values of L_a , D , a , and z_b found from the fit of C_E . The C_1 and C_2 contributions are represented by the dotted and dashed lines, respectively.

$$C_E(\Delta x) = \frac{1}{(1+2\Delta)} \left[\Delta \frac{\sin(k_0 \Delta x)}{k_0 \Delta x} + \frac{J_1(k_0 \Delta x)}{k_0 \Delta x} \right], \quad (6)$$

where k_0 is the free space k vector. This expression gives a good fit over 30 points to the data (Fig. 3) for $\Delta = 0.73$ and $k_0 = 3.6 \text{ cm}^{-1}$, in good agreement with the calculated value at 18 GHz of 3.8 cm^{-1} . This confirms that the scattered intensity angular distribution $I(\theta)$ and the spatial correlation function $C_E(\Delta x)$ are Fourier transforms.

Squaring the field gives the intensity and allows us to compute the intensity correlation function and to compare it to the modulus square of the field correlation function. In the frequency domain, we compare the measured intensity correlation function $C(\Delta \nu)$ to $C_1 + C_2$ given in Eqs. (2) and (A1), assuming C_3 is negligible and using the values of L_a , D , a , and z_b found from the fit to C_E without additional adjustable parameters (Fig. 4). The value $C(\Delta \nu = 0) = 1.13$

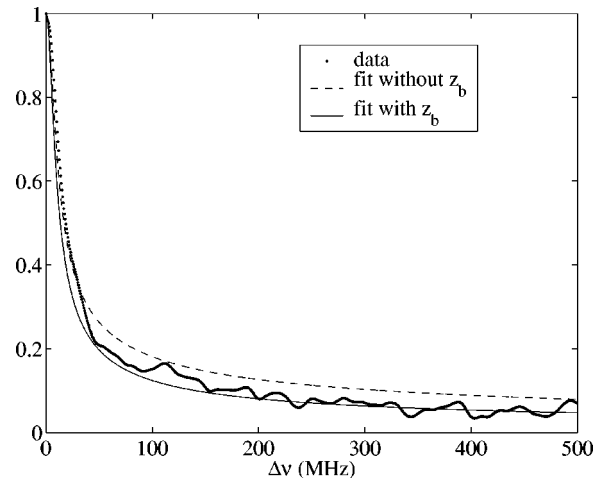


FIG. 5. Long-range contribution to intensity correlation function $C - C_1$ normalized to its value at $\Delta \nu = 0$. The solid line corresponds to Eq. (A1) which includes internal reflection. The dashed line is given by Eq. (3), which does not include internal reflection.

is the variance of the normalized intensity. The difference of this from unity is a measure of mesoscopic corrections to correlation. The $C - C_1$ contribution normalized by its value at $\Delta\nu=0$ is shown in Fig. 5. The comparison to Eq. (A1), which includes z_b , and to Eq. (3) which does not, shows the effect of internal reflection.

In conclusion, we have measured the field correlation function with frequency and displacement and shown that they are the Fourier transforms of the time of flight distribution and the specific intensity, respectively. Comparison with theoretical expressions gives the diffusion coefficient, diffusive absorption length, extrapolation length, and mean free path. The measurement of both the field and intensity correlation functions makes possible a direct separation between short- and long-range intensity correlation.

We are indebted to the late Narciso Garcia for valuable suggestions, support, and encouragement. We thank Professor Boris Shapiro and O. Legrand for helpful discussions and Marin Stoytchev for technical contributions. This work was

supported by the National Science Foundation under Grant Nos. DMR 9973959 and INT9512975, a PSC-CUNY grant, the United States–Israel Binational Science Foundation (BSF), and the Groupements de Recherche POAN and PRIMA.

APPENDIX A

We give the complete expression for the long-range contribution C_2 including absorption and internal reflection, for quasi-one-dimensional geometry. We follow the approach of [40] in which the correlation function was written in the form

$$C_2(\Delta\nu) = 2 \frac{N_a + N_b + N_\alpha}{gBL}, \quad (\text{A1})$$

with an overall factor of 2 to account for the one-channel-in, one-channel-out experimental setup. We obtain the following expressions, which differ for B and N_α from those in [40]:

$$B = [1 + 2z_b^2(\gamma_+^2 - \gamma_-^2) + z_b^4(\gamma_+^2 + \gamma_-^2)^2][\cosh(2\gamma_+L) - \cos(2\gamma_-L)] + 4z_b^2(\gamma_+^2 + \gamma_-^2)[\cosh(2\gamma_+L) + \cos(2\gamma_-L)] \\ + \{4\gamma_+z_b[1 + z_b^2(\gamma_+^2 + \gamma_-^2)]\sinh(2\gamma_+L)\} + \{4\gamma_-z_b[1 - z_b^2(\gamma_+^2 + \gamma_-^2)]\sin(2\gamma_-L)\}, \quad (\text{A2a})$$

$$N_a = \frac{1}{2\gamma_+(\gamma_+^2 - \alpha^2)} \{[(2\gamma_+^2 - \alpha^2) + z_b^2(8\gamma_+^4 + 2\gamma_+^2\gamma_-^2 - \gamma_-^2\alpha^2 - 3\gamma_+^2\alpha^2 + \alpha^4) + z_b^4(\gamma_+^2 + \gamma_-^2)(2\gamma_+^4 - 2\gamma_+^2\alpha^2 \\ + \alpha^4)]\sinh(2\gamma_+L) + [4z_b\gamma_+(3\gamma_+^2 - \alpha^2) + 4z_b^3\gamma_+(3\gamma_+^4 + \gamma_+^2\gamma_-^2 - 2\gamma_+^2\alpha^2 + \alpha^4)]\sinh^2(\gamma_+L)\}, \quad (\text{A2b})$$

$$N_b = \frac{1}{2\gamma_-(\gamma_-^2 + \alpha^2)} \{[-(2\gamma_-^2 + \alpha^2) + z_b^2(8\gamma_-^4 + 2\gamma_+^2\gamma_-^2 + \gamma_+^2\alpha^2 + 3\gamma_-^2\alpha^2 + \alpha^4) - z_b^4(\gamma_+^2 + \gamma_-^2)(2\gamma_-^4 + 2\gamma_-^2\alpha^2 \\ + \alpha^4)]\sin(2\gamma_-L) + [4z_b\gamma_-(3\gamma_-^2 + \alpha^2) - 4z_b^3\gamma_-(3\gamma_-^4 + \gamma_+^2\gamma_-^2 + 2\gamma_-^2\alpha^2 + \alpha^4)]\sin^2(\gamma_-L)\}, \quad (\text{A2c})$$

$$N_\alpha = \frac{\gamma_+^2 + \gamma_-^2}{2\alpha(\gamma_+^2 - \alpha^2)(\gamma_-^2 + \alpha^2)} \{[-\alpha^2 - z_b^2(6\gamma_+^2\gamma_-^2 + 5\gamma_+^2\alpha^2 - 5\gamma_-^2\alpha^2 + \alpha^4) + z_b^4\alpha^2(-2\gamma_+^2\gamma_-^2 - \gamma_+^2\alpha^2 + \gamma_-^2\alpha^2)]\sinh(2\alpha L) \\ + [4z_b\alpha^{-1}(-\gamma_+^2\gamma_-^2 - \gamma_+^2\alpha^2 + \gamma_-^2\alpha^2 - \alpha^4) + 4z_b^3\alpha(-3\gamma_+^2\gamma_-^2 - 2\gamma_+^2\alpha^2 + 2\gamma_-^2\alpha^2)]\sinh^2(\alpha L)\}. \quad (\text{A2d})$$

APPENDIX B

We show that the time of flight distribution and the field correlation function with frequency shift are Fourier transform pairs. The response to a wave packet $f(t)$ is $E(t) = \int d\nu \exp[-i2\pi\nu t]F(\nu)E(\nu)$, where $F(\nu)$ is the Fourier transform of $f(t)$ and $E(\nu)$ is the field measured at a given point at frequency ν . From this expression, the ensemble average of the temporal intensity variation of the transmitted pulse may be written as

$$\langle E^2(t) \rangle = \int d\nu_1 d\nu_2 \exp[-i2\pi(\nu_1 - \nu_2)t] \\ \times \langle E(\nu_1)E^*(\nu_2) \rangle F(\nu_1)F^*(\nu_2). \quad (\text{B1})$$

If $f(t)$ is a short pulse with a bandwidth much wider than the

correlation frequency $\delta\nu$, $F(\nu_1)$ and $F(\nu_2)$ are nearly identical as long as $\nu_2 - \nu_1$ is much smaller than the pulse bandwidth. With the change of variables $\nu_1 = \nu + \Delta\nu/2$ and $\nu_2 = \nu - \Delta\nu/2$, $F(\nu_1)F^*(\nu_2) \approx |F(\nu)|^2$ and Eq. (B1) becomes

$$\langle E^2(t) \rangle = \int d\nu d\Delta\nu \exp[-i2\pi\Delta\nu t] \\ \times \langle E(\nu + \Delta\nu/2)E^*(\nu - \Delta\nu/2) \rangle |F(\nu)|^2. \quad (\text{B2})$$

Within a frequency range in which the variation in the averaged intensity $\langle I(\nu) \rangle$ is small, we can write $\langle E(\nu + \Delta\nu/2)E^*(\nu - \Delta\nu/2) \rangle = \langle I(\nu) \rangle C_E(\nu, \Delta\nu)$, where $C_E(\nu, \Delta\nu)$ is the normalized field correlation function around the frequency ν . In a frequency range in which the change in scattering parameters is small, $C_E(\nu, \Delta\nu) = C_E(\Delta\nu)$, and we find

$$\begin{aligned}
\langle E^2(t) \rangle &= \int d\nu \langle I(\nu) |F(\nu)|^2 \rangle \int d\Delta \nu \\
&\quad \times \exp[-i2\pi\Delta\nu t] C_E(\Delta\nu) \\
&= \int_0^\infty dt \langle I(t) \rangle \int d\Delta \nu \exp[-i2\pi\Delta\nu t] C_E(\Delta\nu),
\end{aligned}
\tag{B3}$$

where the last step follows from Parseval's theorem. Consequently, the time of flight distribution $\mathcal{I}(t) = \langle E^2(t) \rangle / \int dt \langle I(t) \rangle$ and the field correlation function are Fourier transform pairs:

$$\mathcal{I}(t) = \int d\Delta \nu C_E(\Delta\nu) \exp[-i2\pi\Delta\nu t].
\tag{B4}$$

-
- [1] J. W. Goodman, *Statistical Optics* (John Wiley, New York, 1985).
- [2] A. A. Chabanov and A. Z. Genack, *Phys. Rev. E* **56**, R1338 (1997).
- [3] J. W. Goodman, in *Laser Speckle and Related Phenomena*, Vol. 9 of *Topics in Applied Physics*, edited by J. C. Dainty (Springer-Verlag, Berlin, 1984), pp. 9–75.
- [4] B. Shapiro, *Phys. Rev. Lett.* **57**, 2168 (1986).
- [5] N. Garcia and A. Genack, *Phys. Rev. Lett.* **63**, 1678 (1989).
- [6] A. Z. Genack and N. Garcia, *Europhys. Lett.* **21**, 753 (1993).
- [7] M. Stoytchev and A. Z. Genack, *Opt. Lett.* **24**, 262 (1999).
- [8] M. C. W. van Rossum and T. M. Nieuwenhuizen, *Rev. Mod. Phys.* **71**, 313 (1999).
- [9] E. Kogan and M. Kaveh, *Phys. Rev. B* **52**, R3813 (1995).
- [10] V. Fal'ko and K. Efetov, *Phys. Rev. B* **52**, 17 413 (1995).
- [11] M. J. Stephen and G. Cwilich, *Phys. Rev. Lett.* **59**, 285 (1987).
- [12] S. Feng, C. Kane, P. A. Lee, and A. D. Stone, *Phys. Rev. Lett.* **61**, 834 (1988).
- [13] R. Berkovits and S. Feng, *Phys. Rep.* **238**, 135 (1994).
- [14] M. P. van Albada, J. F. de Boer, and A. Lagendijk, *Phys. Rev. Lett.* **64**, 2787 (1990).
- [15] J. F. de Boer, M. P. van Albada, and A. Lagendijk, *Phys. Rev. B* **45**, 658 (1992).
- [16] J. F. de Boer, M. C. W. van Rossum, M. P. van Albada, T. M. Nieuwenhuizen, and A. Lagendijk, *Phys. Rev. Lett.* **73**, 2567 (1994).
- [17] M. Stoytchev and A. Z. Genack, *Phys. Rev. Lett.* **79**, 309 (1997).
- [18] R. A. Webb, S. Washburn, C. P. Umbach, and R. B. Laibowitz, *Phys. Rev. Lett.* **54**, 2696 (1985).
- [19] P. A. Lee and A. D. Stone, *Phys. Rev. Lett.* **55**, 1622 (1985).
- [20] B. A. Altshuler and D. E. Khmel'nitskii, *Pis'ma Zh. Eksp. Teor. Fiz.* **42**, 291 (1985) [*JETP Lett.* **42**, 359 (1985)].
- [21] B. L. Altshuler, V. E. Kravtsov, and I. V. Lerner, in *Mesosopic Phenomena in Solids*, edited by B. L. Altshuler, P. A. Lee, and R. A. Webb (North-Holland, Amsterdam, 1991).
- [22] V. Prigodin, K. Efetov, and S. Iida, *Phys. Rev. Lett.* **71**, 1230 (1993).
- [23] A. Z. Genack, N. Garcia, and W. Polkosnik, *Phys. Rev. Lett.* **65**, 2129 (1990).
- [24] P. A. Mello, *Phys. Rev. Lett.* **60**, 1089 (1988).
- [25] P. A. Mello, E. Akkermans, and B. Shapiro, *Phys. Rev. Lett.* **61**, 459 (1988).
- [26] A. Z. Genack and J. M. Drake, *Europhys. Lett.* **11**, 331 (1990).
- [27] A. Z. Genack, in *The Scattering and Localization of Classical Waves*, edited by P. Sheng (World Scientific, Singapore, 1990), pp. 70–74.
- [28] R. Pnini and B. Shapiro, *Phys. Rev. B* **39**, 6986 (1989).
- [29] N. Garcia, A. Z. Genack, R. Pnini, and B. Shapiro, *Phys. Lett. A* **176**, 458 (1993).
- [30] A. Lagendijk, R. Vreeker, and P. de Vries, *Phys. Lett. A* **136**, 81 (1989).
- [31] J. X. Zhu, D. J. Pine, and D. A. Weitz, *Phys. Rev. A* **44**, 3948 (1991).
- [32] A. Z. Genack, J. H. Li, N. Garcia, and A. A. Lisyansky, in *Photonic Band Gaps and Localization*, edited by C. M. Soukoulis (Plenum Press, New York, 1993), p. 23.
- [33] R. Pnini and B. Shapiro, *Phys. Lett. A* **157**, 265 (1991).
- [34] E. Kogan and M. Kaveh, *Phys. Rev. B* **45**, 1049 (1992).
- [35] F. Scheffold and G. Maret, *Phys. Rev. Lett.* **81**, 5800 (1998).
- [36] B. A. van Tiggelen, P. Sebbah, M. Stoytchev, and A. Z. Genack, *Phys. Rev. E* **59**, 7166 (1999).
- [37] I. Freund, M. Rosenbluh, and S. Feng, *Phys. Rev. Lett.* **61**, 2328 (1988).
- [38] J. H. Li and A. Z. Genack, *Phys. Rev. E* **49**, 4530 (1994).
- [39] I. Freund and D. Eliyahu, *Phys. Rev. A* **45**, 6133 (1992).
- [40] M. C. W. van Rossum and T. M. Nieuwenhuizen, *Phys. Lett. A* **177**, 452 (1993).